DIALKOXYETHANE–PROPYLENE CARBONATE MIXED ELECTROLYTES FOR LITHIUM SECONDARY BATTERIES

SHIN-ICHI TOBISHIMA, JUN-ICHI YAMAKI, AKIHIKO YAMAJI and TAKESHI OKADA

Ibaraki Electrical Communication Laboratory, Nippon Telegraph and Telephone Public Corporation, Tokai, Ibaraki-ken, 319-11 (Japan)

(Received November 13, 1983; accepted June 11, 1984)

Summary

The electrolytic characteristics of various 1,2-dialkoxyethane (DAE)–propylene carbonate (PC) mixed solvent electrolytes for Li secondary batteries have been examined. DAE[$H_3C(CH_2)_nOC_2H_4O(CH_2)_nCH_3$] is a low viscous, non-cyclic, aprotic solvent. As DAEs, dimethoxyethane (DME), diethoxyethane (DEE), and dibutoxyethane (DBE) were used. The conductivities of PC/DME and of PC/DEE showed maximum values around PC/DAE volume ratios of 1/1 and at 1M solute, due mainly to the high dielectric constant of PC and the low viscosity of DAE. The Li^+ ion conductivity changed according to the DAE molecular volume. 1M $LiAsF_6$–PC/DME (1/1) showed an approximately 2.6 times higher conductivity, 13.8×10^{-3} ohm^{-1} cm^{-1}, than PC alone. Lithium charge–discharge efficiency on the Li substrate increased with decreasing reactivity between Li and DAE, which would be expected from the oxidation potential for DAE. $LiClO_4$–PC/DME and PC/DEE showed a greater than 90% Li cycling efficiency.

1. Introduction

Mixed solvent systems have been considered as electrolytic solutions for Li primary and/or secondary batteries. The conductivities of mixed solvent electrolytes, such as $LiClO_4$–propylene carbonate (PC) mixed with 1,2-dimethoxyethane [1, 2], and with 12-crown-4 [3], have been reported. However, their Li charge–discharge characteristics have not been studied in depth. We have previously reported on the Li^+ ion conductivity and on Li cycling behavior in $LiClO_4$–PC mixed with cosolvents (which selectively solvate Li^+ ion) such as tetrahydrofuran [4] and *N,N,N′,N′*-tetramethylethylenediamine [5]. We here report the electrolyte properties of PC mixed with 1,2-dialkoxyethane (DAE). DAEs have low viscosity and are non-cyclic, aprotic solvents. The structure below and Table 1 show the general formula and physical properties of DAEs. In this work, 1,2-dimethoxyethane (DME), 1,2-diethoxyethane (DEE) and 1,2-dibutoxyethane (DBE) were examined.

0378-7753/84/$3.00

$$\begin{array}{ll} CH_2O(CH_2)_nCH_3 & n = 0, \text{DME} \\ | & n = 1, \text{DEE} \\ CH_2O(CH_2)_nCH_3 & n = 3, \text{DBE} \end{array}$$

TABLE 1

Physical properties of DAE [6]

Solvent	Boiling point (°C)	Melting point (°C)	Dielectric constant at 25 °C	Viscosity at 20 °C (cP)
DME	85.2	−70	5.5	0.48*
DEE	121.4	−74	5.1	0.65
DBE	203.3	−69.1	—	1.34
PC	242.0	−48.8	69.0	2.50

*From ref. 7.

2. Experimental

2.1. Electrolytes

PC (Tokyo Kasei Co.) was distilled at approximately 4 mmHg pressure and 108 °C. DME was distilled with NaH at normal pressure and 85 °C after pre-treatment with KOH for a few days. High-grade distilled DEE and DBE (Tomiyama Pure Chemicals Ind. Co.) were used. $LiClO_4$ (Kanto Chemicals Co.) and $LiBF_4$ (Morita Chemicals Co.) were employed after drying under vacuum at 160 °C and 100 °C, respectively. $LiAsF_6$ (United States Steel, Agri Chemicals Co.) was used as received. Electrolytic solutions were prepared by mixing adequate amounts of solute and solvents at room temperature. The water contents of the electrolytes were measured using the Karl Fischer method and found to be less than 100 ppm. PC/DBE mixed solvents separated into two phases at more than 50% DBE content. Compositions for the two phases were determined by gas chromatography. The upper phase was a DBE-rich phase. The lower phase was used as the measurement sample after the composition was calibrated by gas chromatography.

2.2. Measurements

Lithium charge–discharge tests were galvanostatically carried out on conductive substrates (Al, Pt, Ni and Cu: 99.99%, Fru-uchi Chemicals Co.) with a Rauh type cell [8], shown in Fig. 1. This cell, with approximately 2 ml of solution, was constructed with an Li counter electrode (20 mm dia. × 0.5 mm), an Li reference electrode, and the conductive substrate working electrode (20 mm dia. × 0.5 mm). The working electrodes were used after polishing with emery paper and rinsing with PC. The lithium charge–discharge efficiency was obtained from the stripping charge/plating charge at 0.8 V potential cut-off as the stripping end point [9]. Lithium cycling tests on the Li substrate (Li-on-Li cycling) [10] were carried out using the cell men-

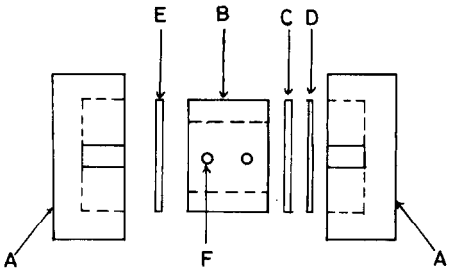

Fig. 1. Test cell for Li cycling [8]. A, Teflon end pieces; B, cylindrical Teflon center piece; C, Li disk (counter electrode); D, Ni screen contact; E, Pt disk (working electrode); F, reference electrode and filling holes.

tioned above. This experiment involved pre-plating the Pt substrate with Li at 2.4 C/cm^2, followed by stripping, and then re-plating at 0.6 C/cm^2 (0.5 mA/cm^2) on the pre-plated Li. The average efficiency per cycle, E_a, is calculated from eqn. (1).

$$E_a = \frac{Q_{ps} - Q_{ex}/n}{Q_{ps}} \times 100(\%) \tag{1}$$

where n is the number of apparent "100%" cycles, Q_{ps} is the charge stripped (0.6 C/cm^2) and Q_{ex} is the charge in the excess Li (1.8 C/cm^2) at the start of the experiment.

The solvent oxidation potentials were measured by potential linear sweep (1 - 10 V sweep, 20 mV/s), using a Teflon cell with a Pt working electrode (0.32 cm^2), an Li reference electrode, and an Li counter electrode (1 cm^2) [11]. The oxidation potentials reported are those at which the current reached 1 mA on the working electrode. The transport number for Li^+ (t_o^+) was obtained from the electromotive force of a concentration cell [2]. The Stokes' radius for Li^+ (r_{so}^+), the practical ion radius with solvated solvent molecules, was calculated from Stokes' law shown in eqn. (2) [12]. This value was calibrated by a method using a series of tetraalkylammonium ions [12]. The solvation number (S_{NO}^+) was calculated using r_{so}^+, the Li^+ crystal radius (r_c^+) and the solvent molecular volume (V_s) from eqn. (3) [2].

$$r_{so}^+ = \frac{|z_i|F^2}{6\Pi\eta_o\Lambda_o t_o^+ N} \tag{2}$$

where z_i, F, N and Λ_o represent the ionic charge, the Faraday constant, the Avogadro number and the infinite molar equivalent conductivity, respectively.

$$S_{NO}^+ = \frac{4\pi(r_{so}^{+3} - r_c^{+3})}{3V_s} \tag{3}$$

The solvent viscosities (η_o) were measured using an Ubbelohde-type viscometer at 25 °C. Electrolyte preparations and all the tests were carried out in an Ar-filled drybox at 25 ± 1 °C.

Scanning electron microscope (SEM) studies on the deposited Li were carried out as follows: lithium was deposited on the Al holder for SEM observation (the deposited surface area was approximately 0.13 cm^2) and the deposited lithium was rinsed with dehydrated DME in the Ar-filled drybox. The sample, in a glass case, was transferred to a second drybox which was connected to the pre-vacuum sample chamber of the JSM-T JEOL scanning microscope.

3. Results and discussion

3.1. Electrolyte conductivity for $LiClO_4$–PC/DAE

Figure 2 shows the conductivity (κ) dependence on the DAE content for 1M $LiClO_4$–PC/DAE. For PC/DME and PC/DEE (curves (a) and (b) in Fig. 2) the conductivities reached their maximum values (κ_{max}) at a PC/DAE volume ratio of 1/1. For PC/DBE, the conductivity showed a slightly higher value than for PC, above PC/DBE = 1/1. These conductivity enhancements resulted from the effects of both the high dielectric constant of PC and the low viscosity of DAE, which resulted in a better ion dissociation and enhanced ion migration than those observed in single solvent systems [2].

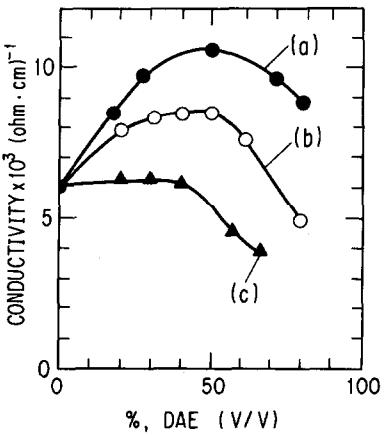

Fig. 2. Conductivity for 1M $LiClO_4$–PC/DAE. (a) PC/DME; (b) PC/DEE; (c) PC/DBE.

Figure 3 shows the conductivity dependence on $LiClO_4$ concentration for PC/DAE systems. The conductivities showed maximum values at about 1M solute. In PC/DME (Fig. 3, curve (a)), higher conductivities, greater than 10^{-2} ohm^{-1} cm^{-1}, were obtained in the 0.8 - 2.0M range, due to the low viscosity, while for PC alone the conductivity rapidly decreased at greater than 1M. The maximum conductivity order for $LiClO_4$–PC/DAE was PC/DME > PC/DEE > PC/DBE ≈ PC. The conductivity for 1M $LiClO_4$–PC/DME (1/1), 10.5×10^{-3} ohm^{-1} cm^{-1}, was approximately 75% greater than in PC.

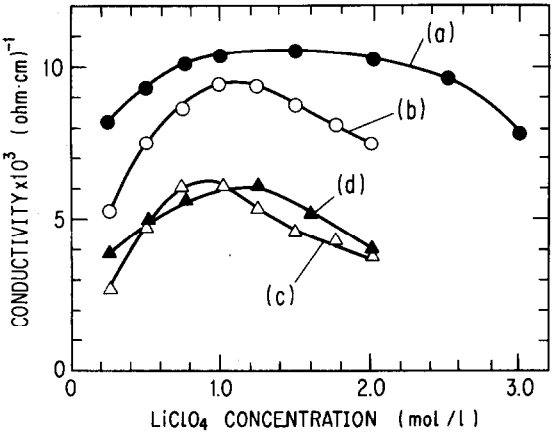

Fig. 3. Conductivity for $LiClO_4$–PC/DAE. (a) PC/DME (1/1); (b) PC/DEE (1/1); (c) PC/DBE (6/4); (d) PC.

TABLE 2

Conductivity and electrolyte parameters for $LiClO_4$–PC/DAE

Solvents	$\kappa_{max} \times 10^3$ (ohm^{-1} cm^{-1})	Λ_0 (ohm^{-1} cm^2 mol^{-1})	t_0^+	η_0 (cP)	r_{so}^+ (Å)	V_s (Å^3)	S_{NO}^+
PC/DME (1/1)	10.5	61.5	0.45	1.2	3.9	172.4	1.5
PC/DEE (1/1)	8.6	48.0	0.27	1.5	4.6	233.2	1.7
PC/DBE (6/4)	6.2	31.5	0.13	2.2	6.1	345.7	2.8
PC alone	6.0	27.0	0.32	2.5	4.4	140.5	2.5

κ_{max}, maximum conductivity; Λ_0, limiting molar conductivity;
t_0^+, transport number for Li^+ ion; η_0, viscosity for solvents;
V_s, solvent molecular volume for DAE and PC; r_{so}^+, calibrated Stokes radius for Li^+ ion;
S_{NO}^+: solvation number for Li^+ ion.

To evaluate the conductivity enhancement mechanism, electrolytic parameters, such as the transport number, were measured. Table 2 shows the limiting molar conductivity (Λ_o), the solvent viscosities (η_o), the solvent molecular volumes (V_S), the transport number (t_o^+), Stokes' radius (r_{so}^+) and the solvation number (S_{NO}^+) for Li^+ in $LiClO_4$–PC/DAE systems under infinite dilution conditions where the anion effect can be neglected [2]. Because DAE selectively solvates Li^+ ion in PC/DAE [2, 13], we only used the V_s value of DAE for the calculation of S_{NO}^+ in $LiClO_4$–PC/DAE. Λ_o for PC/DAE was higher than for PC alone due to the lower viscosity, as shown in Table 2. The values of t_0^+ and $1/r_{so}^+$ were in the order of PC/DME > PC > PC/DEE > PC/DBE. These may be explained as follows:

(i) DAE has a stronger solvation power for cations than PC [2, 13] and the addition of DAE causes Li^+–DAE complex formation, as in the case of tetrahydrofuran [5].

(ii) For DAE groups, the solvation power for cations increases with increasing carbon number, because the electron density on the oxygen atoms of the alkoxy groups increases with the increase in the electron induction effect of the alkyl groups [14].

(iii) The solvent molecular volume also increases with increasing carbon atoms, as shown in Table 2.

Summarizing the three tendencies mentioned above, the practical Li^+ radius increases with the increase in carbon numbers for DAE. Therefore, the size of the solvated Li^+ was of the order of PC/DME > PC > PC/DEE > PC/DBE.

3.2. Lithium charge–discharge characteristics for $LiClO_4$–PC/DAE

Lithium cyling tests on the Li substrate (Li-on-Li cycling) were performed galvanostatically for $LiClO_4$–PC/DAE, where Q_{ex} = 1.8 C/cm^2, Q_{ps} = 0.6 C/cm^2 and the current density was 0.5 mA/cm^2. Figure 4 shows the average Li cycling efficiency (E_a) dependence on the DAE content for 1M $LiClO_4$–PC/DAE. E_a values increased to a maximum around PC/DAE = 1/1.

Figure 5 shows the E_a dependence on the $LiClO_4$ concentration for PC/DAE. The values showed maxima at about 1M. In PC/DME, on going

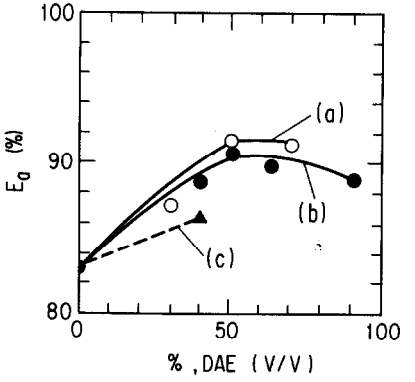

Fig. 4. Lithium cycling efficiency for 1M $LiClO_4$–PC/DAE. Q_{ex} = 1.8 C/cm^2, Q_{ps} = 0.6 C/cm^2, I_{ps} = 0.5 mA/cm^2. (a) PC/DEE; (b) PC/DME; (c) PC/DBE.

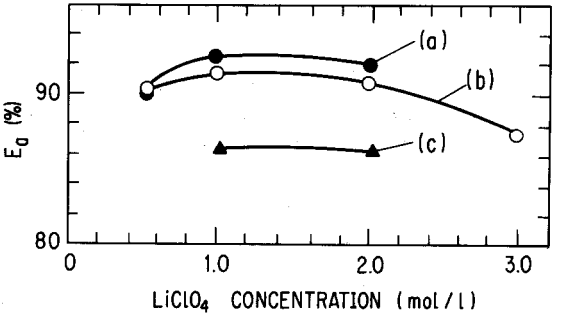

Fig. 5. Lithium cycling efficiency for $LiClO_4$–PC/DAE. Q_{ex} = 1.8 C/cm^2, Q_{ps} = 0.6 C/cm^2, I_{ps} = 0.5 mA/cm^2. (a) PC/DEE (1/1); (b) PC/DME (1/1); (c) PC/DBE (6/4).

from 1.0 to 2.0M $LiClO_4$, optimal E_a values (>90%) were obtained. These tendencies, shown both in Figs. 4 and 5, were similar to those observed for electrolyte conductivity.

Table 3 summarizes the E_a values for 1M $LiClO_4$–PC/DAE. The E_a order was PC/DEE > PC/DME > PC/DBE > PC. The E_a for PC/DEE was slightly higher than for PC/DME.

TABLE 3

Li cycling efficiency for 1M $LiClO_4$–PC/DAE

Solvents	E_a (%)
DEE/PC (1:1)	91.2
DME/PC (1:1)	90.6
DBE/PC (4/6)	86.4
PC alone	83.3

Q_{ex} = 1.8 C/cm^2; Q_{ps} = 0.6 C/cm^2, 0.5 mA/cm^2.

Figure 6 shows the relation between E_a and the oxidation potentials for DAE. The E_a values increased with decreasing oxidation potential for the solvent; *i.e.*, decreasing the reduction reactivity of the solvent by Li [15, 16]. These results agree with published reports that a decrease in stripping efficiency results mainly from solvent reduction by the activated, deposited Li [10, 16]. The E_a order between DME and DEE also agrees with the alkali metal stability in DME and DEE [17].

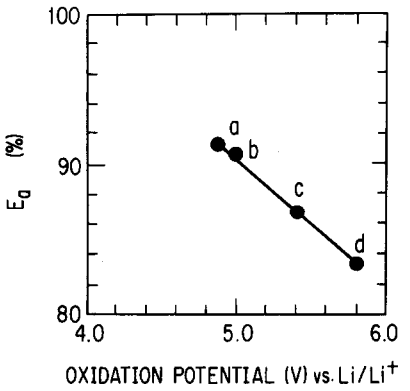

Fig. 6. Relation between E_a and oxidation potential for DAE and PC; 1M $LiClO_4$. (a) PC/DEE (1/1); (b) PC/DME (1/1); (c) PC/DBE (6/4); (d) PC.

From these results, we believe that the solvated Li^+ adsorbs on the Li electrode and the high solvation tendency for DAE causes a DAE-rich layer on the Li surface.

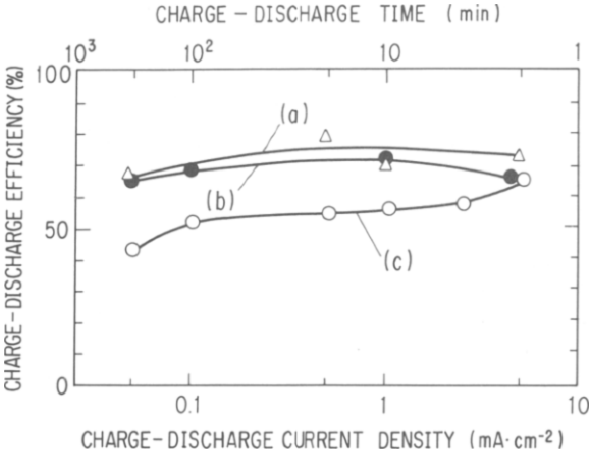

Fig. 7. Lithium cycling efficiency dependence on current density at 0.6 C/cm^2 on the Pt working electrode; 1M $LiClO_4$. (a) PC/DEE (1/1); (b) PC/DME (1/1); (c) PC.

Figure 7 shows Li charge–discharge efficiency dependence on charge–discharge current density (I_{ps}) at a constant capacity. Efficiency is reported as the first cycle value obtained from the stripping charge/plating charge on the Pt working electrode. Efficiency decreased with decreasing I_{ps} (charge–discharge time increasing) in PC alone, as shown in curve (c) of Fig. 7. Otherwise, efficiencies for PC/DEE and PC/DME (Fig. 7, curves (a) and (b), respectively) were higher than in PC and the efficiency decrease with change in I_{ps} was much smaller than for PC alone. These results also indicate that Li reactivity for PC/DEE and PC/DME is less than for PC [4, 18] and they agree with the results for Li-on-Li cycling.

In order to examine the morphology of the lithium deposition, SEM studies were carried out for $LiClO_4$–PC/DME. The results are shown in Fig. 8. For PC (Fig. 8(a)), lithium deposited as a fibrous dendrite layer, as

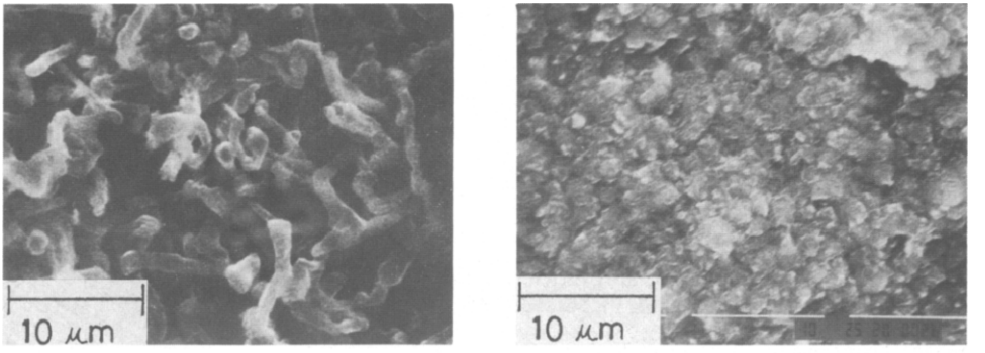

Fig. 8. Morphology of deposited Li on Al at 3.6 C/cm^2, 1 mA/cm^2 (×3500). (a) 1M $LiClO_4$–PC; (b) 1M $LiClO_4$–PC/DME (1/1).

reported previously [19]. The dendritic nature of the Li layer has been reported as being due to only partial electrical contact of the deposited metal because of the PC–Li reaction [10]. For PC/DME (Fig. 8(b)), a more compact layer was formed. The reasons for this behavior are, possibly:

(i) better electrical contact than for PC due to lower reactivity between Li and DME, or

(ii) a different kind of film formation on the Li, and/or

(iii) higher Li^+ concentration around the deposited lithium.

Summarizing the results for both Li^+ ion conductivity and Li cycling efficiency, PC/DME is the most preferable of the PC/DAE mixed systems examined in this work. More experiments were therefore carried out on the PC/DME systems.

3.3. Characteristics of LiX–PC/DME

In this section, the effects of solutes and substrates were examined when cycling Li in PC/DME.

3.3.1. Conductivity

Conductivities were measured for PC/DME (1/1) incorporating $LiAsF_6$, $LiClO_4$ and $LiBF_4$. The results are shown in Table 4. For all the solutes, the conductivities of PC/DME were higher than those of PC alone. The conductivity order for PC/DME was $LiAsF_6 > LiClO_4 > LiBF_4$. This order is the same as that for the anion radius, as shown in Table 4. The reason for this agreement is that the solute with the larger anion is affected more by the ion migration rate (solvent viscosity) than by ion dissociation (solvent dielectric constant). The solute with the larger anion has the stronger dissociation power (the coulombic force between Li^+ and X^- is smaller). Therefore, the conductivity order is as mentioned above.

TABLE 4

Conductivity for 1M LiX–PC/DME (1:1)

Solute	Conductivity × 10^3 ($ohm^{-1}\ cm^{-1}$)		Anion radius* (Å)
	PC/DME	PC	
$LiAsF_6$	13.4	5.3	3.26
$LiClO_4$	10.5	6.0	2.83
$LiBF_4$	7.8	3.9	2.78

*Calculated from ref. 24.

3.3.2. Lithium cycling characteristics

The dependences of Li cycling efficiency on the solutes and on the plating substrate were examined for PC/DME. The results are shown in Table 5. For the solute effects, the 10th average Li cycling efficiency ($E_{ff,10}$) followed the order of $LiClO_4 > LiAsF_6 > LiBF_4$. The effects of $LiAsF_6$ were

TABLE 5

Li cycling efficiency for 1M LiX–PC/DME (1/1) at 0.5 mA/cm^2 current density and 0.6 C/cm^2 charge density

Solute	$E_{ff,10}$ (%)			
	Substrate			
	Al (92)*	Pt (80)*	Ni (50)*	Cu (42)*
$LiClO_4$	79 [85]**	70 [86]**	50	36
$LiAsF_6$	75 [76]**	68 [76]**	45	36
$LiBF_4$	70 [74]**	57 [72]**	48	—

*Electrochemical alloying efficiency reported in ref. 22.
**First cycle efficiency.

less than expected. $LiAsF_6$ was reported to be effective on Li cycling by Li^+ ion conductive film formation resulting from the $LiAsF_6^-$ reaction [10]. However, this mechanism causes a rapid decrease in Li cycling efficiency with cycling [20, 21].

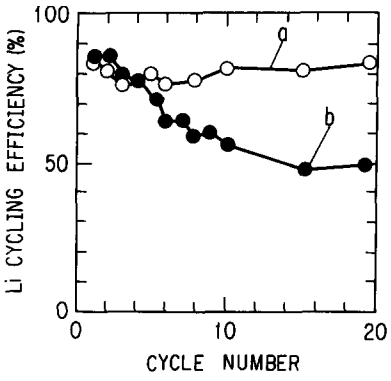

Fig. 9. Relation between Li cycling efficiency and cycle number at 0.5 mA/cm^2, 0.6 C/cm^2 for 1M $LiClO_4$–PC/DME (1/1). (a) on Al; (b) on Pt.

For the substrate effects, the $E_{ff,10}$ order was Al > Pt > Ni > Cu. The first cycle efficiency did not differ significantly between that of Al and Pt. However, as seen in Fig. 9, with increasing cycle number the efficiency on Pt decreased more rapidly than that on Al. These facts suggest that the substrate effects are connected with electrochemical Li alloying. $E_{ff,10}$ values increased with increasing electrochemical alloying efficiency, as reported by Dey [22]. Electrochemical alloying may lead to a decrease in the reactivity between Li and solvents, and/or lead to the adherence of deposited Li on alloying substrates [23].

4. Conclusion

Electrolyte characteristics were examined for PC/DAE mixed solvent systems. The overall conductivity, κ, of PC electrolyte systems was increased by the addition of DAE. However, Li^+ ion conductivity was found to depend on DAE molecular volume, as well as on the dielectric constant and viscosity. Lithium cycling efficiency increased with decreasing reactivity between Li and DAE, which is expected from the oxidation potential for DAE. Considering both Li^+ ion conductivity and Li cycling efficiency, PC/DME was found to be the most preferable of the PC/DAE systems investigated in this study, for use in Li secondary batteries.

Acknowledgement

The authors express their gratitude to Mr C. Uemura for his helpful guidance and discussion during the course of this research.

References

1 Y. Matsuda and H. Satake, *J. Electrochem. Soc., 127* (1980) 8777.
2 Y. Matsuda, H. Nakashima, M. Morita and Y. Takasu, *J. Electrochem. Soc., 128* (1981) 2552.
3 I. A. Angres, *Abstract No. 42,* The Electrochem. Soc. Fall Meeting Extended Abstracts, Vol. 80-7, 1980, pp. 113 - 114.
4 S. Tobishima and A. Yamaji, *Electrochim. Acta, 28* (1983) 1067.
5 S. Tobishima and A. Yamaji, *J. Power Sources, 12* (1984) 53.
6 T. Asakura (ed.), *Solvent Handbook,* Kodansha Inc., Japan, 1976, pp. 478 - 482; 485 - 493.
7 J. A. Riddick and W. B. Burger, *Organic Solvents,* Wiley–Interscience, New York, 3rd Edn., 1970, p. 34.
8 R. D. Rauh, T. F. Reise and S. B. Brummer, *J. Electrochem. Soc., 125* (1978) 186.
9 R. D. Rauh and S. B. Brummer, *Electrochim. Acta, 22* (1977) 75.
10 V. R. Koch, *J. Power Sources, 6* (1981) 357.
11 S. Tobishima and A. Yamaji, *Electrochim. Acta, 29* (1984) 267.
12 R. A. Robinson and R. H. Stokes, *Electrolyte Solutions,* Butterworths, London, 1955, pp. 116 - 124.
13 U. Mayer, *Proc. Lithium Nonaqueous Battery Electrochemistry,* The Electrochem. Soc. Inc., New Jersey, 1980, p. 13.
14 D. J. Cram and G. S. Hammond, *Organic Chemistry,* McGraw-Hill, New York, 1964, pp. 206 - 209.
15 V. R. Koch, J. L. Goldman, C. J. Mottos and M. Mulvaney, *J. Electrochem. Soc., 129* (1982) 1.
16 J. L. Goldman, R. M. Mank, J. H. Young and V. R. Koch, *J. Electrochem. Soc., 127* (1980) 1461.
17 A. H. Saadi and W. H. Lee, *J. Chem. Soc. (B),* (1966) 1.
18 R. Selim and P. Bro, *J. Electrochem. Soc., 121* (1974) 1457.
19 J. Rene van Beek and P. J. Rommers, in J. Thompson (ed.), *Power Sources 7,* Academic Press, London, 1978, p. 595.
20 A. J. Parker, P. Singh and E. J. Frazer, *J. Power Sources, 10* (1983) 1.
21 V. R. Koch and S. B. Brummer, *Electrochim. Acta, 23* (1978) 55.
22 A. N. Dey, *J. Electrochem. Soc., 118* (1971) 1547.
23 M. Garreau, J. Thevenin and M. Fekir, *J. Power Sources, 9* (1983) 235.
24 T. Kunitake, Y. Matsunaga and C. Aso, *Polym. J., 2* (1971) 345.